JCTC Journal of Chemical Theory and Computation

Energy Conservation in Adaptive Hybrid Atomistic/ Coarse-Grain Molecular Dynamics

Bernd Ensing,*,† Steven O. Nielsen,‡ Preston B. Moore,§ Michael L. Klein,|| and Michele Parrinello†

Department of Chemistry and Applied Biosciences, ETH Zurich USI-Campus, Via Giuseppe Buffi 13, Lugano, CH-6900 Switzerland, Department of Chemistry, University of Texas at Dallas, 2601 North Floyd Road, Richardson, Texas 75083-0688, Department of Chemistry and Biochemistry, University of the Sciences in Philadelphia, Philadelphia, Pennsylvania 19104, and Center for Molecular Modeling, Department of Chemistry, University of Pennsylvania, Philadelphia Pennsylvania 19104-6323

Received November 3, 2006

Abstract: Multiscale computer simulation algorithms are required to describe complex molecular systems with events occurring over a range of time and length scales. True multiscale simulations must solve the interface, or hand-shaking, problem of coupling together different levels of description in different spatial regions of the system. If the spatial regions of different resolution move over time, or if material is allowed to flow over the inter-region boundaries, a mechanism must be introduced into the multiscale algorithm to allow material to dynamically change its representation. While such a mechanism is highly desirable in many instances, it is fraught with technical difficulties. Here, we present a molecular dynamics simulation algorithm which is multiscale in both time and space. We supplement the potential and kinetic energy expressions with auxiliary terms in order to recover the total energy as a conserved quantity, even when the total number of degrees of freedom changes during the simulation. This is crucial for a proper assessment of the quality of adaptive hybrid algorithms, and in particular, it allows us to tune the hierarchy of RESPA levels to optimize the integration scheme.

I. Introduction

In computer simulation, multiscale methods break the calculation up into parts to be treated at different levels of resolution or accuracy. Multiscale methods are therefore more economical, allowing for larger systems, longer time scales, or simply less resources than calculations performed entirely at the most demanding level. An example of a successful multiscale approach in molecular simulation is the quantum mechanical/molecular mechanical (QM/MM) treatment of enzymatic proteins, in which the chemically active region of the enzyme is modeled with an accurate QM method, while the remaining protein scaffold and the aqueous environment are described with a classical MM force field.[1,2]

In this paper, we present a hybrid atomistic/coarse-grain molecular dynamics method which allows parts of a molecular system to be simulated in full atomistic detail while treating the rest of the system at a coarse-grain (CG) resolution. Here, CG refers to a dimensional reduction by lumping atoms together into single interaction sites, that way drastically reducing the number of particles and pair interactions in the calculation. CG simulations can therefore access much longer time scales and larger system sizes than canonical molecular dynamics (MD) and has found successful application in the modeling of polymer melts,[3,4] biomembranes,[5] and proteins.[6,7]

The idea of combining an atomistic with a lower-resolution description is not new. Carloni et al. joined atomistic MD with a Go-type of model for the simulation of proteins,[8,11]

* Corresponding author e-mail: bernd.ensing@phys.chem.ethz.ch.
† ETH Zurich USI-Campus.
‡ University of Texas at Dallas.
§ University of the Sciences in Philadelphia.
|| University of Pennsylvania.

10.1021/ct600323n CCC: $37.00
Published on Web 03/28/2007

while Koumoutsakos et al. linked atomistic MD to a continuum description to model nanoscale fluid mechanics.[12] Kurkcuoglu et al. studied protein motions at mixed levels of coarse-graining within an elastic network approach,[9] and Voth et al. used a force-field-fitting approach to parametrize atom−CG bead interactions in a mixed atomistic and coarse-grained MD simulation.[10] A particularly advantageous approach was recently introduced by Kremer et al. which allows particles to change their representation from atomistic to CG and vice versa during a MD simulation,[13,14] while Abrams presented a similar adaptive dual-resolution method within a Monte Carlo approach.[15]

It is important that molecules can adapt their representation when they diffuse over the region boundaries in order to maintain the spatial separation in regions of different resolution. On very short time scales and in rigid molecular systems, such diffusion is minimal, so that a nonadaptive approach can be sufficient. This is often the case in the aforementioned QM/MM simulation of enzymes. On the other hand, when the chemical (QM-treated) region is solvent-exposed and protons or water molecules take part in the chemistry, MM-treated water molecules can replace the QM ones, so that the chemistry is not correctly described unless the representation adapts. Also, when the phenomenon of high-resolution interest displaces through the system, an adaptive scheme is required. The QM/MM treatment of the propagation of a crack in a brittle solid, in which only the atoms in the advancing crack tip region are modeled at the QM tight-binding level of theory, is an example of such an adaptive approach.[16]

In the case of an atomistic/CG molecular dynamics treatment, the method is especially aimed to study molecular motions on long time scales, making it natural to seek an adaptive algorithm. Coarse-graining is typically applied to model soft matter, and the range of phenomena in this field that could be studied with an adaptive hybrid atomistic/coarse-grained description is only limited by our imagination but could include diffusion of molecules and ions in swollen polymers, conformational dynamics in proteins, ligand docking, physisorption at a solid/liquid interface, permeation and diffusion in biomembranes, and so forth.

To set up a (particle-based) dual-resolution simulation, the system is, arbitrarily, spatially divided into a high-resolution atomistic region (AR) and a low-resolution CG region (CGR). For example, the AR can be defined within a sphere of fixed-radius centered on a specific particle. This way, the AR follows the tagged particle and evolves when particles move through the spherical boundary. A standard force field can be employed for the evolution of the individual atoms in the AR, whereas the particles in the CGR are evolved using a CG force field—for example, one fitted against the atomistic force field using force-matching methods[17,18] or inverse Monte Carlo techniques.[19] The coupling between the two regions is done at the CG level by first mapping the AR into its CG representation (which involves grouping the atoms into larger particles) and then evaluating the cross interactions with the CG force field, after which the effective forces on the CG particles in the AR are distributed mass-weighted over their constituent atoms.[13]

Difficulties arise when particles are allowed to diffuse over the regional boundaries and change their atomistic/coarse-grain (A/CG) representation on the fly. In particular, instantaneous switching of the atomistic potentials into the CG ones or vice versa would cause spurious jumps in the forces and velocities of the particles. Instead, the discontinuity between the AR and CGR is bridged by an intermediate *healing region* (HR), in which crossing particles gradually acquire their new representation. In the scheme of Kremer et al., this is done using force scaling.[13] Instead, here, we will scale the potentials, the advantages of which are the main focus of this paper. Second, we exploit the reversible RESPA multi-time-step approach,[20] evaluating rapidly oscillating forces, such as those arising from bond interactions between atoms, more frequently than the slowly fluctuating nonbonded forces. The natural hierarchy of RESPA levels commonly employed in atomistic simulations generalizes in a straightforward manner to the A/CG situation, allowing us to tune the molecular dynamics integrator optimally across the entire system.

II. Method

The present hybrid scheme assigns both atomistic and coarse-grain positions and velocities throughout the entire system. Given an atomistic configuration and a CG mapping (i.e., a grouping of the atoms into CG particles), the coarse-grained representation is readily computed, taking for each CG position the center of mass of its constituent atoms and likewise for the velocities. Recently, some of us developed an efficient algorithm to obtain an atomistic configuration from a CG one, the so-called inverse mapping, which is not straightforward because of missing information.[21] Molecules in the AR and HR are evolved at the atomistic level, and their CG positions (and velocities) are updated in the RESPA substep for the evaluation of the inter-region interactions. In the CGR, the CG particles are evolved, and their corresponding atomistic positions and velocities are frozen relative to these centers.

The accuracy of the integration of the equations of motion (i.e., the quality of the simulation) is evaluated by monitoring the total energy, which is a conserved quantity of the system. The total energy in a hybrid system is composed of the sum of kinetic and potential energies of the distinct spatial regions, plus the energy that is exchanged with extended variables (e.g., those of a thermostat), plus the change in kinetic and potential energies due to particles that adapt their resolution.

The total kinetic energy, K, is

$$K = \sum_{\alpha\in(\mathrm{AR,HR})} \sum_{i\in\alpha} \frac{p_i^{\,2}}{2m_i} + \sum_{\alpha\in\mathrm{CGR}} \frac{p_\alpha^{\,2}}{2M_\alpha} + \Delta K_\alpha^{\mathrm{A/CG}} \qquad (1)$$

where, for each CG particle α in the AR and HR, we sum the kinetic energy of its constituent atoms, i (with p the momentum and m the mass), and for each CG particle in the CGR, its kinetic energy, plus an extra term $\Delta K^{\mathrm{A/CG}}$:

$$\Delta K_\alpha^{\mathrm{A/CG}} = \sum_{i\in\alpha} \frac{\tilde{p}_i^{\,2}}{2m_i} - \frac{\tilde{p}_\alpha^{\,2}}{2M_\alpha} \qquad (2)$$

This term is the surplus kinetic energy that is associated with the atomistic representation of a CG particle but which is "integrated out" upon coarse-graining. Its value is computed at the start of the simulation and is then updated whenever a particle α crosses the CGR/HR boundary, adding or subtracting the kinetic energy difference between the two representations of the particle. To distinguish the momenta in eq 2 from the normal instantaneous momenta in eq 1, we add here and hereafter a tilde to indicate a book-keeping property that is only updated upon adaptation of a particle's resolution and frozen in between.

The potential-energy function is separated into interactions that are confined between sites within a single CG particle and interactions between sites spanning more than one CG particle. The first type of interactions, termed *intra-CG particle* interactions and shown in eq 3, consists of atomistic potentials, Φ_{ij}, where i and j are atoms belonging to the same CG particle α. They are evaluated in the AR and HR but not in the CGR where the atoms are frozen with respect to the CG particle they are associated with. Similar to the kinetic energy, an extra term, $\Delta W^{\text{intraCG}}$, arises to account for this frozen inherent atomistic potential energy, $\tilde{\Phi}$, within each CG particle in the CGR; its value is recorded at the start of the simulation, after which it is updated whenever a particle crosses the CGR/HR boundary.

$$V^{\text{intraCG}} = \sum_{\alpha\in(\text{AR,HR})} \sum_{\substack{i\in\alpha \\ j\in\alpha}} \Phi_{ij} + \sum_{\alpha\in(\text{CGR})} \Delta W_\alpha^{\text{intraCG}} \qquad (3)$$

$$\Delta W_\alpha^{\text{intraCG}} = \sum_{\substack{i\in\alpha \\ j\in\alpha}} \tilde{\Phi}_{ij} \qquad (4)$$

All other interactions, termed *inter-CG particle* interactions, are governed by eq 5. That is, the interaction between CG particles α and β is composed of the scaled CG potential $\Phi_{\alpha\beta}$ and the scaled atomistic interactions Φ_{ij} between atoms i and j belonging to α and β, respectively, with the scaling factor λ a number between 0 and 1.

$$V^{\text{interCG}} = \sum_\alpha \{ \sum_{\beta>\alpha} \lambda_{\alpha\beta}\Phi_{\alpha\beta} + \sum_{\beta>\alpha} (1-\lambda_{\alpha\beta}) \sum_{\substack{i\in\alpha \\ j\in\alpha}} \Phi_{ij} + \Delta W_\alpha^{\text{interCG}} \} \qquad (5)$$

Equation 5 also contains an extra term, $\Delta W^{\text{interCG}}$, that accounts for the changes in V^{interCG} when particles change their A/CG character.

For an infinitely thin HR, the scaling factor, λ, becomes simply a Heaviside step function, Θ, that is equal to unity if one or both particles are in the CGR and is equal to 0 otherwise. In such a case of instantaneous resolution switching, $\Delta W^{\text{interCG}}$ can be explicitly expressed and computed as the energy difference in V^{interCG} when particle α crosses the region boundary, analogous to the auxiliary terms in eqs 2 and 4:

$$\Delta W_\alpha^{\text{interCG}} = \Theta \sum_\alpha (\tilde{\Phi}_{\alpha\beta} - \sum_{\substack{i\in\alpha \\ j\in\alpha}} \tilde{\Phi}_{ij}) \qquad (6)$$

Note however that, contrary to the other two auxiliary terms

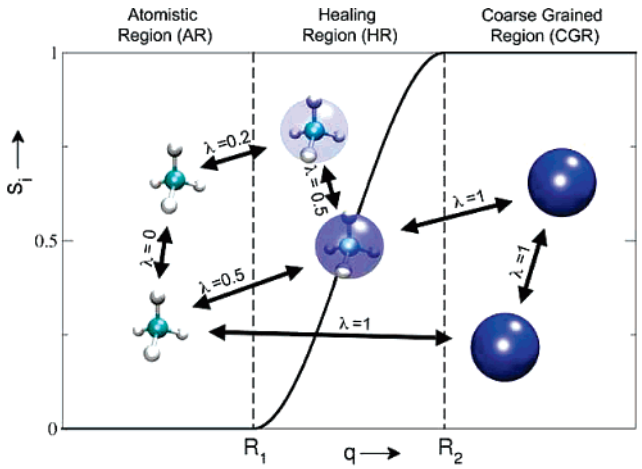

Figure 1. Switch function s shown as a function of an arbitrary distance q. Here, $s = 0$ for each CG particle (and its atoms) within a sphere $q < R1$ (atomistic region) and $s = 1$ for particles outside $q > R2$ (coarse-grained region). Pair interactions are scaled by $\lambda = \max[s_1,s_2]$.

$\Delta K_\alpha^{\text{A/CG}}$ and $\Delta W_\alpha^{\text{intraCG}}$, which are local and consist of constant (frozen) intra-CG atomistic contributions of particles in the CGR, evaluation of $\Delta W^{\text{interCG}}$ requires nonlocal information including inter-CG atomistic interactions that are not constant, which would nullify the efficiency of the CG representation. That is, we can indeed store that part of the kinetic and potential energies that become inherent to the CG bead when a particle α moves from the AR to the CGR by taking the energy difference (using eqs 2, 4, and 6), but when this particle returns to the AR and the inherent energies become explicit again, $\Delta W_\alpha^{\text{interCG}}$ is of course not the same as when it left the AR, thus rendering the absolute value of $\Delta W_\alpha^{\text{interCG}}$ meaningless. Instead, we will only book-keep the changes to this term when molecules change representation, where we make use of a smoothly changing scaling function, λ, in the HR in the following manner.

The scaling factor is equal to

$$\lambda_{\alpha\beta} = \max[s(\mathbf{r}_\alpha), s(\mathbf{r}_\beta)] \qquad (7)$$

where s_α is the fraction of CG character of particle α, which depends on its position $\mathbf{r}$ relative to the regional boundaries as illustrated in Figure 1. For particles in the AR, s is 0; in the CGR, s is 1, and in the HR, s has an intermediate value, signifying a hybrid character. Here, we take s to be a simple polynomial function of the distance q between the particle and a fixed position that smoothly switches from 0 to 1 between the AR/HR boundary at R_1 and the HR/CGR boundary at R_2:

$$s_\alpha(q) = \begin{cases} 0 & \text{if } q < R_1 \\ (q-R_1)^2(3R_2 - R_1 - 2q)/(R_2-R_1)^3 & \text{if } R_1 \le q \le R_2 \\ 1 & \text{if } q > R_2 \end{cases} \qquad (8)$$

Let us consider for a moment the forces on the particles by taking the derivatives of the potential $V = V^{\text{intraCG}} + V^{\text{interCG}}$, namely eq 3 plus eq 5. The derivatives of the first part give

the usual contributions to the forces; however, applying the chain rule to the scaled potentials in V^{interCG} results in forces of the following shape:

$$f_\alpha = -\lambda(\mathbf{r}_\alpha,\mathbf{r}_\beta)\frac{\partial\Phi(\mathbf{r}_\alpha,\mathbf{r}_\beta)}{\partial\mathbf{r}_\alpha} - \frac{\partial\lambda(\mathbf{r}_\alpha,\mathbf{r}_\beta)}{\partial\mathbf{r}_\alpha}\Phi(\mathbf{r}_\alpha,\mathbf{r}_\beta) - \ldots \quad (9)$$

Here, the usual forces $\partial\Phi/\partial\mathbf{r}_\alpha$ are recognized in the first term, scaled by λ, but the second term introduces a new force, consisting of the derivative of the scaling function multiplied by the potential. This term is only nonzero for particles in the HR and gives rise to a force on these particles that changes their A/CG character, $s(\mathbf{r})$, which is seen to be spurious.

To understand the origin of this new force, consider an atomistic torsion potential, $V_{ijkl}^{\text{dihedral}}$, spanning two CG particles ($i, j \in \alpha$, and $k, l \in \beta$) located in the HR. The molecule can now lose this torsional potential energy in two ways: (1) by gaining kinetic energy in the usual physical manner via a motion in the direction of the first term in eq 9 or 2 by moving in the direction of the second term (i.e., toward the CGR) so that the potential is scaled down to 0. The second term thus causes a spurious flux of particles through the HR. Note, however, that the loss of the atomistic torsional potential energy that causes this force should be canceled by CG potential terms (on average) and that any instantaneous differences should be taken as inherent CG energy, stored in $\Delta W^{\text{interCG}}$. In other words, even though we do not have an explicit expression for $\Delta W^{\text{interCG}}$ in the case of smoothly scaled potentials, we can keep track of the energy flow from and to $\Delta W^{\text{interCG}}$ because we know its derivative as minus the second term in eq 9.[22]

With the second term in the force expression canceled, only the first term, namely, the scaled force, is left in the equations of motion. To obtain the total energy, however, we need to accurately book-keep the amount of nonlocal "inter-GC particle" potential energy that transfers from explicit (atomistic) into the inherent CG term, $\Delta W^{\text{interCG}}$. This is done in a manner analogous to the thermodynamic integration applied in free-energy perturbation methods. That is, the energy flow is evaluated by integration of the derivative of W^{interCG} (i.e., minus the second term in eq 9) on the fly for particles moving in the HR:

$$\Delta\Delta W^{\text{interCG}} = \int_{\Delta\mathbf{r}} \sum_{\substack{\alpha\in\text{HR}\\ \beta\in\text{AA,HR}}} \Phi(\mathbf{r})\frac{\mathrm{d}\lambda}{\mathrm{d}\mathbf{r}}\mathrm{d}\mathbf{r}' \approx \sum_t \sum_{\substack{\alpha\in\text{HR}\\ \beta\in\text{AA,HR}}} \Phi(\mathbf{r})\frac{\mathrm{d}s(q_\alpha)}{\mathrm{d}q_\alpha}\Delta q_\alpha \qquad s_\alpha > s_\beta \quad (10)$$

where the sum runs over all scaled inter-CG interactions (including the atomistic ones) between CG particles α and β and the integral is approximated by a Riemann's sum over time steps t, making use of the fact that the change in λ equals the change in s of the particle (α) with maximum s (see eq 7). Here, Δq is the displacement of the particle in the direction of changing s (i.e., toward or from the CGR).

The main function of the HR is to facilitate the introduction of atomistic detail when a CG particle leaves the CGR. Without a HR, instantaneous switching to the atomistic interactions would lead to large repulsive forces due to overlaps of the nonequilibrated atoms. Rather, the atomistic interactions are turned on gradually across the width of the healing region. In addition, many-body interactions, such as bend and torsion potentials spanning more than one CG particle, are evaluated as in eq 5, where λ is determined by the particle with the maximum CG character.

All particles are coupled to individual Nose−Hoover thermostat chains, which are frozen when the particles are not explicitly evolved upon crossing regional boundaries (namely, for CG particles in the AR and HR and for atoms in the CGR). Coupling of the atoms to thermostats in the healing region is particularly important for two reasons. First, the particles that leave the CGR have atomistic velocities that were stored from the last time they left the AR (or were drawn from a random distribution at time zero) and, thus, need to be updated before entering the AR. Second, the atomistic positions of such particles also need to be equilibrated because these particles tend to be too high on the atomistic potential energy surface. This excess potential energy is transformed into kinetic energy while the atoms cross the HR heading toward the AR, which is conveniently removed with a thermostat. Consequently, we expect to see a decreasing $\Delta W^{\text{interCG}}$, as molecules moving from the CGR toward the AR on average have a higher atomistic potential than molecules moving in the opposite direction (e.g., consider also the case of eq 6), with a slope with opposite sign and equal magnitude as the potential energy of the thermostat (see the Supporting Information for an illustration). The requirement of thermostats excludes the calculation of transport properties, although in principle, it is possible to only couple particles in the HR to a thermostat and reduce the influence on the dynamics in the other regions.

In the rest of this paper, we will illustrate the method by applying it to two model systems: first, a single two-particle molecule moving across the regional boundaries and, second, a periodic box of dense methane.

III. Applications

A. Simple Bead and Spring Molecule Changing Representation. Figure 2 illustrates the first application, namely, a single molecule that is represented at both the atomistic and CG levels by two atoms connected with a bond. The only difference is the force constant of the harmonic bond potential, which is 10 times smaller in the CGR than in the AR. The AR is a two-dimensional slab of thickness $2r_{\text{AR}} = 10$ Å, flanked on both sides by a 5-Å-thick HR and an outer CGR. The cubic box with edge length $L = 30$ Å is subject to periodic boundary conditions, and the molecule has a velocity parallel to the AR slab normal vector that takes it 6 ps to move through the entire box. The $\Delta K^{\text{A/CG}}$ and $\Delta W^{\text{intraCG}}$ terms are 0 in this special case of a one-to-one mapping, and the remaining nonzero $\Delta W^{\text{interCG}}$ term allows us to test the integration scheme. The solid black lines show the total energy (with and without the correction) when the molecule is oriented with the bond stretch vibration perpendicular to the velocity, while the red lines show the energies in the case of parallel orientation (see also the yellow inset). The dashed lines show the correction, W^{interCG}. The inset in the

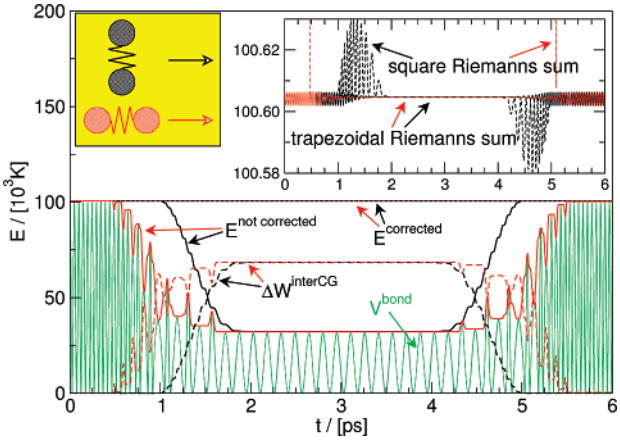

Figure 2. Total energy of a two-atom molecule that moves from the AR via a HR into the CGR (where the bond is 10× weaker) and back. Black lines: molecule orientation perpendicular to its velocity. Red lines: parallel orientation (see the yellow inset). Green line: potential energy during the parallel orientation trajectory. The inset shows the superiority of the trapezoidal Riemann's sum (eq 11).

upper right-hand corner of Figure 2 zooms in on the fluctuations of the total energy, showing strong oscillations when the integral is estimated by the straightforward rectangular Riemann's sum of eq 10, which uses only the end-point evaluation of the function on the interval Δq (not taking into account the "midpoint rule" of integration). Much better total energy conservation is obtained by including the function value at the start point of the time-step interval and taking the average (making use of the "trapezoid rule"):

$$\Delta\Delta W^{\text{interCG}} = \sum_t \sum_{\substack{\alpha\in\text{HR} \\ \beta\in\text{AA,HR}}} \frac{1}{2}\left[\Phi_t(\mathbf{r})\frac{ds_t(q_\alpha)}{dq_\alpha} + \Phi_{t-1}(\mathbf{r})\frac{ds_{t-1}(q_\alpha)}{dq_\alpha}\right]\Delta q_\alpha \qquad s_\alpha > s_\beta \quad (11)$$

Clearly, the integration scheme works to recover the total energy as a conserved quantity in this example of adaptive hybrid MD.

B. Hybrid Molecular Dynamics of Liquid Methane. The second, more realistic, illustration is a cubic box containing 8000 methane molecules. The box has an edge length of 79.9 Å and is subject to periodic boundary conditions. In a spherical AR with a radius of 8 Å, the CH_4 molecules are represented in atomistic detail with flexible bonds and bends.[23] The AR is surrounded by a 4-Å-thick spherical healing region. Both regions are centered on a noninteracting dummy particle that is fixed in space, but in other test simulations, we have also used a methane molecule to center these regions, in which case the AR and HR follow the motion of that methane molecule. In the outlying CGR, the molecules are represented by a single van der Waals sphere using Jorgensen's united atom model.[24] The density of methane in this setup is 0.418 g/mL, which is close to the actual density of liquid methane (at 1 atm and 111.5 K) of 0.423 g/mL.

The multi-time-step approach is employed with an outer time step of 2 fs and substeps in which the CG long-range van der Waals interactions are updated once, the CG short-range Van der Waals interactions twice, the atomistic long-range and short-range van der Waals and electrostatics twice and four times, respectively, and the bond and bend interactions 32 times (for further details, see the Supporting Information). A further speedup is gained by treating the periodic boundary conditions for the AR and HR in the CG representation, which is allowed when the longest distance in those regions is smaller than half of the shortest box edge. For systems with charged CG particles, the long-range electrostatics are taken into account using Ewald summation at the CG level.

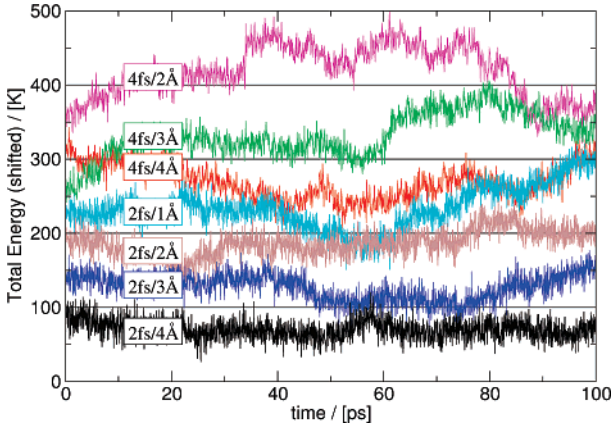

Figure 3. Total energies (shifted for comparison) of hybrid MD simulations of 8000 methane molecules, using different time steps and healing region widths. The energy is well-conserved using a time step of 2 fs and a HR width of 4 Å.

As seen in the first example above, the best total energy conservation is reached by averaging $\Phi d\lambda/dq$ in the integration scheme (eq 11). Implemented in that form, however, requires storing $\Phi d\lambda/dq$ of the previous time step $(t - 1)$ for all scaled interactions. Instead, we can rewrite eq 11 in sums of $\Phi d\lambda/dq$ that have the same displacement Δq. The displacement is determined by the interacting particle with the maximum CG character, so that the number of terms to be stored is only as large as the number of CG particles in the HR.

In Figure 3, the total energy from the first 100 ps of this hybrid MD simulation is compared with those from hybrid simulations using different outer time steps and different HR widths. A clear trend can be observed of total energy conservation improvement with decreasing time-step and increasing HR-width.

Further details on the analysis of a 600 ps trajectory of the best combination are found in the Supporting Information. The numbers of methane molecules in the AR, HR, and CGR were 34.0 ± 2.3, 77.5 ± 3.8, and 7889.4 ± 3.8, respectively. The radial distribution functions, mean square displacements, and velocity autocorrelation functions of the hybrid MD simulation averaged over the methane atoms in the AR show excellent agreement with those from a purely atomistic MD simulation of a box of 1000 methane molecules.

IV. Conclusions

We have presented a hybrid atomistic/CG MD method that allows particles to change resolution on the fly. By introduc-

ing auxiliary terms to the kinetic and potential energy expressions, we recover the total energy as a conserved quantity, even when the total number of degrees of freedom changes during the simulation. These auxiliary energy terms should be seen as the inherent energy of the CG particles that is "integrated out" upon the dimensional reduction and becomes explicit again when switching back to the atomistic representation. Using a reversible RESPA multistep integration scheme, our method has the benefits of being truly multiscale in both time and space. Conserving energy is particularly important in hybrid MD, as it is the fundamental property used to evaluate the choice of the subtime steps and the size of the intermediate healing region with respect to the quality of the simulation. In particular for hybrid MD simulations of more complex systems than methane, in which case it is expected that a wider healing region is required, we now have the machinery in place to assess the quality of hybrid MD.

Supporting Information Available: Technical details and analysis of the hybrid MD simulation of methane, including a short illustrative mpeg movie. This material is available free of charge via the Internet at http:///pubs.acs.org.

References

(1) Carloni, P.; Rothlisberger, U.; Parrinello, M. *Acc. Chem. Res.* **2002**, *35*, 455.

(2) Warshel, A. *Annu. Rev. Biophys. Biomol. Struct.* **2003**, *32*, 425.

(3) Baschnagel, J.; Binder, K.; Doruker, P.; Gusev, A. A.; Hahn, O.; Kremer, K.; Mattice, W. L.; Muller-Plathe, F.; Murat, M.; Paul, W.; Santos, S.; Suter, U. W.; Tries, V. *Adv. Polym. Sci.* **2000**, *152*, 41.

(4) Muller-Plathe, F. *Chem. Phys. Chem.* **2002**, *3*, 754.

(5) Nielsen, S. O.; Lopez, C. F.; Srinivas, S.; Klein, M. L. *J. Phys.: Condens. Matter* **2004**, *16*, R481.

(6) Go, N. *Annu. Rev. Biophys. Bioeng.* **1983**, *12*, 183.

(7) Brown, S.; Fawzi, N. J.; Head-Gordon, T. *Proc. Natl. Acad. Sci. U.S.A.* **2003**, *100*, 10712.

(8) Neri, M.; Anselmi, C.; Cascella, M.; Maritan, A.; Carloni, P. *Phys. Rev. Lett.* **2005**, *95*, 218102.

(9) Kurkcuoglu, O; Jernigan, R. L.; Doruker, P. *Polymer* **2004**, *45*, 649.

(10) Shi, Q.; Izvekov, S.; Voth, G. A. *J. Phys. Chem. B* **2006**, *110*, 15045.

(11) Neri, M.; Anselmi, C.; Carnevale, V.; Vargiu, A. V.; Carloni, P. *J. Phys.: Condens. Matter* **2006**, *18*, S347.

(12) Werder, T.; Walther, J. H.; Koumoutsakos, P. *J. Comput. Phys.* **2005**, *205*, 373.

(13) Praprotnik, M.; Delle Site, L.; Kremer, K. *J. Chem. Phys.* **2005**, *123*, 224106.

(14) Praprotnik, M.; Delle Site, L.; Kremer, K. *Phys. Rev. E: Stat., Nonlinear, Soft Matter Phys.* **2006**, *73*, 066701.

(15) Abrams, C. *J. Chem. Phys.* **2005**, *123*, 234101.

(16) Csányi, G.; Albaret, T.; Payne, M. C.; DeVita, A. *Phys. Rev. Lett.* **2004**, *93*, 175503.

(17) Ercolessi, F. Adams, J. B. *Europhys. Lett.* **1994**, *26*, 583.

(18) Izvekov, S.; Parrinello, M.; Burnham, C. J.; Voth, G. *J. Chem. Phys.* **2004**, *120*, 10896.

(19) Lyubartsev, A. P.; Laaksonen, A. *Phys. Rev. E: Stat., Nonlinear, Soft Matter Phys.* **1995**, *52*, 3730.

(20) Tuckerman, M.; Berne, B. J.; Martyna, G. J. *J. Chem. Phys.* **1992**, *97*, 1990.

(21) Nielsen, S. O.; Ensing, B.; Moore, P. B.; Klein, M. L. Coarse Grain to Atomistic Mapping Algorithm: A Tool for Multiscale Simulations. In *Advances in Hierarchical and Multi-Scale Simulations of Materials*; Mohanty, S., Ross, R. B., Eds.; Publisher: Taylor and Francis: Oxford, U. K., 2006; in press.

(22) This is easily shown to be true in the infinitely thin HR case for which we have an explicit expression for $\Delta W^{\text{interCG}}$ (eq 6), and the forces are thus given by $f_\alpha = -\Theta(q - R_2)(\partial\Phi/\partial\mathbf{r}) - \Phi[\partial\Theta(q - R_2)/\partial\mathbf{r}] - \Theta(-q + R_2)(\partial\tilde{\Phi}/\partial\mathbf{r}) - \tilde{\Phi}[\partial\Theta(-q + R_2)/\partial\mathbf{r}]$. Indeed, the second term is canceled by the derivative of $\Delta W^{\text{interCG}}$ (third and fourth terms), because the third term is zero in all regions and the fourth term equals minus the second term, as the derivative of the Heaviside step function is the δ function, $\delta(q - R_2)$, which equals unity at the HR/CG boundary R_2 where $\Phi = \tilde{\Phi}$ and zero otherwise.

(23) Sun, Y.; Spellmeyer, D.; Pearlman, D. A.; Kollman, P. *J. Am. Chem. Soc.* **1992**, *114*, 6798.

(24) Jorgensen, W.; Madura, J.; Swenson, C. *J. Am. Chem. Soc.* **1984**, *106*, 6638.

CT600323N